

Taylor Impact of Fibre Reinforced Concrete Bars.

Jaroslav Buchar^{a*}, Jan Trnka^a, Martina Drdlová^b

^aInstitute of Thermomechanics Czech Academy of Sciences, Prague, Czech Republic

^bResearch Institute of Building Materials, Hnevkovskeho 65, Brno, Czech Republic

ABSTRACT: The impact resistance of fibre reinforced concrete was investigated using a Taylor impact test. Striking velocities up to 31 m/s were applied. The four types of fibre were used: carbon, polypropylene, aramid and wollastonite. The results showed that the dynamic compressive strength increased with the striking velocity. The highest rate sensitivity was reported for carbon and polypropylene fibres. The addition of aramid fibres did not lead to the increase of the compressive strength in comparison with the unreinforced concrete. The dynamic compressive strength lies between static compressive strength and the dynamic strength evaluated using a Split Hopkinson Pressure Bar technique. Qualitative features of the specimen damage were studied using high speed camera.

KEY WORDS: Taylor test, concrete, reinforcing fibres, compressive strength, strain rate sensitivity, high speed camera

Date of Submission: 05-12-2020

Date of acceptance: 20-12-2020

I. INTRODUCTION.

Concrete – like materials (concrete, mortar, and geo-materials) are widely used in civil and military engineering structures. These structures might be exposed to the intensive dynamic loads (e.g. explosions and impact). The understanding of the mechanical properties of these materials is just subject of a great interest. It is well known that the concrete – like materials exhibit significant brittleness which increases with the increasing loading rate (strain or stress rate). The reduction of the brittleness may be achieved by the addition of fibres to concrete [1-3]. The mechanical properties of the fibre reinforced concrete under impact loading are reviewed in [4]. In this paper the main experimental methods used for the material response to the dynamic loading are reviewed, including methods based on stress wave propagation, in which a stress wave is generated and propagated through a long steel bar and impacts the specimens (i.e., the Split Hopkinson pressure bar (SHPB) test [5,6]).

In the given paper the experimental procedure known as the Taylor test is used for the study of high strain rate behaviour of fibre reinforced concrete. The original Taylor test consists in the axial impact of a cylindrical rod against a flat rigid anvil. [7]. This technique is widely used to study the deformation and fracture behaviour of materials at large strains and rates of strain up to 10^5 s^{-1} , and to provide data for the validation of constitutive and failure algorithms used in numerical codes. This experimental method is used mostly for the high strain rate testing of metallic materials [8, 9] and polymers [10-12]. The use of this method in the study of dynamic response of brittle materials to impact loading is very limited, e.g. this method is not involved in the review of experimental methods used for the testing of dynamic behaviour of brittle materials [13]. There are only some papers dealing with the deformation and fracture behaviour of glasses [14, 15] [and ceramics [16].

The aim of the present paper is to study fracture behaviour of fibre reinforced concrete materials using the Taylor test and the comparison of these results with previous achievements obtained using the most common tests like dynamic compression of the specimens using the Hopkinson Split Pressure Bar [17] and dynamic tension using the indirect tensile test (Brazilian test) [18]. The concrete specimens with carbon, aramid, polypropylene and wollastonite fibers have been tested. The details of the specimen damage development during the Taylor test were studied using the high speed camera.

II. MATERIAL AND EXPERIMENTAL PROCEDURE.

For the experiments specimens with various dispersed micro-fibre reinforcement were prepared. The basic material consists of fine SiO_2 sand with grain size of 0 – 0.5 mm, cement CEM 52.5R and water. Superplasticizer Glenium 422 was added to achieve good workability with low water/binder ratio. High dosage of

silica fume Elkem 940U was used to reach an optimum of packing density. The composition of this basic mixture is given in the Table I.

Table I. The composition of the basic mixture (MATERIAL REF).

Cement (kgm ⁻³)	CEM 52.5R	SiO ₂ (kgm ⁻³)	Silica fume (kgm ⁻³)	Superplastizer (kgm ⁻³)	Water (kgm ⁻³)
990		670	78	10	320

The used fibres and their amount in particular composite are described in the Table II.

Table II. Composites description.

Composite designation	Fibre	Fibre amount (vol %)	Length/Diameter of the fibre (mm/ μ m)	Fibre density (kgm ⁻³)
MATERIAL A	aramid	1.5	1/12	1400
MATERIAL C	Carbon PAN	1.5	2/12	1760
MATERIAL P	Polypropylene	1.5	2.2/15	910
MATERIAL W	Wollastonite	2.0	0.3/9	2800

The details of mixing procedure are described e.g. in [16].

The mechanical parameters – compressive and flexural strength were obtained using universal strength testing machine TIRAtest 2710, R58/02. The compressive and flexural load was applied in quasi-static conditions at the speed of 5 mm/min. The dynamic mechanical properties were obtained using of the Hopkinson Split Pressure Bar technique (HSPBT). This experimental technique was also used for the evaluation of the tensile – splitting strength. Detail description of this procedure can be found in [16, 20].

For Taylor test experiments the cylindrical specimen (15 mm in diameter and 50 mm in length) were cast. The specimens were striking against an elastic bar instead of a rigid anvil as in the classical Taylor test. This experimental arrangement is also known as Taylor cylinder – Hopkinson bar impact experiment [20]. The experimental set up is shown in the Fig.1. This arrangement enables to record a time history of the stress originated from the specimen impact.

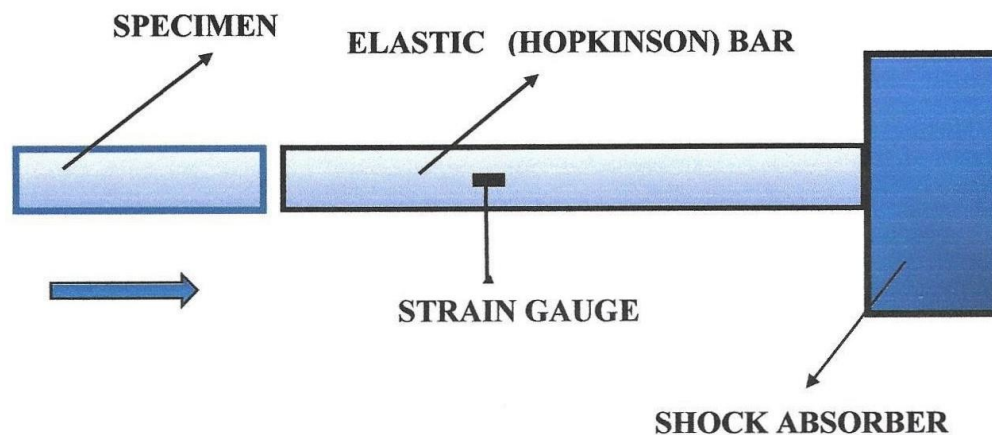


Figure1: Schematic of the experimental set – up.

The recorded stress pulse $\sigma_I(t)$ is characterized by the following main parameters:

Maximum of the stress (amplitude) σ_{Im}

Impulse $I = \int_0^\lambda \sigma_I(t) dt$, where λ is the stress pulse duration

Energy of the stress pulse $w_I = \frac{1}{Z} \int_0^\lambda \sigma_I^2(t) dt$, where Z is the acoustic impedance of the bar ($Z =$ material density \times longitudinal elastic wave velocity).

In our experiments the bar was 1000 mm long, 15 mm in diameter and made from the high strength steel, $Z = 40.8425$ MPas/m.

In order to obtain information on the specimen behavior impacts themselves were monitored by high speed photography, using PHOTRON FASTCAM SA-Z type 2100K-M, Frame Rate 210000fps, Shutter Speed 1.00 μ s and Resolution 384x160 dpi. All experiments were performed at the room temperature.

III. RESULTS AND DISCUSSION.

In this study, a total of 31 experiments were conducted on fibre reinforced concrete rods. These rods (specimens) were striking against the elastic bar. Striking velocities up to 31 m/s were used. Immediately after a Taylor impact a longitudinal stress wave is formed and propagates both into the elastic (Hopkinson) bar and into the specimen. This wave is recorded in the Hopkinson bar which remains in one - dimensional stress state. As described e.g. in [14], in Taylor experiments the material undergoes a transition from an initial one - dimensional strain at the impact face, to a state of one - dimensional stress. The specimen (rod) response to the impact starts as elastic. The maximum stress (amplitude) of this wave increases with the increase in striking velocity. If the stress is large enough the specimen damage starts at the interface between the specimen and Hopkinson bar. The compressive stress pulse in the specimen propagates to its free end. Its reflection causes tensile wave to be generated which can cause tensile damage known as spalling [21].

In the Fig.2 example of the experimental records of the stress pulses σ_I obtained for different striking velocities is displayed.

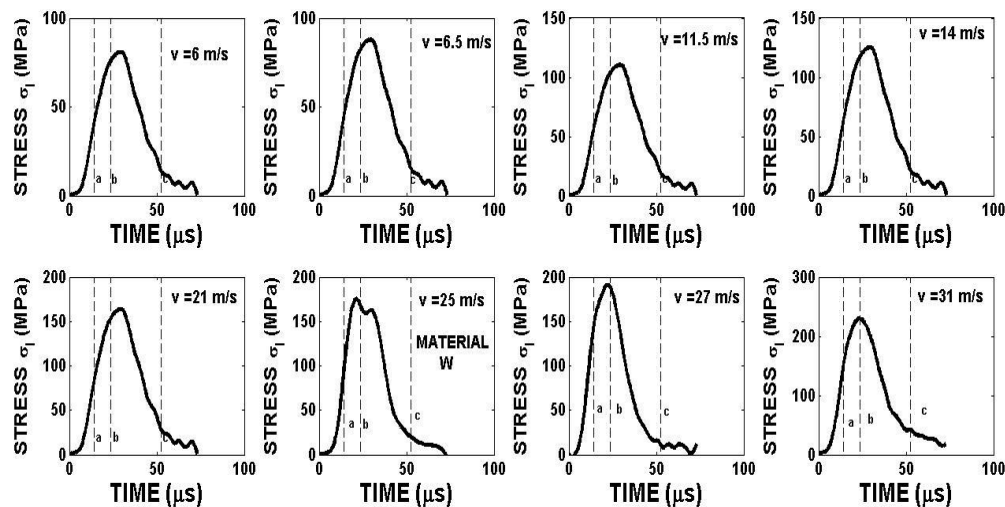


Figure 2: Time histories of the stress pulses σ_I (t) recorded in the Hopkinson bar for different striking velocities of the specimen impact. Material W.

It can be seen that the increase in the striking velocity leads to the increase in the maximum of the stress (amplitude). The qualitative feature of the stress pulse remains unchanged with an exception of the striking velocity =25 m/s.

The stress pulses recorded during the Taylor impact tests for all tested materials are presented in the Fig.3.

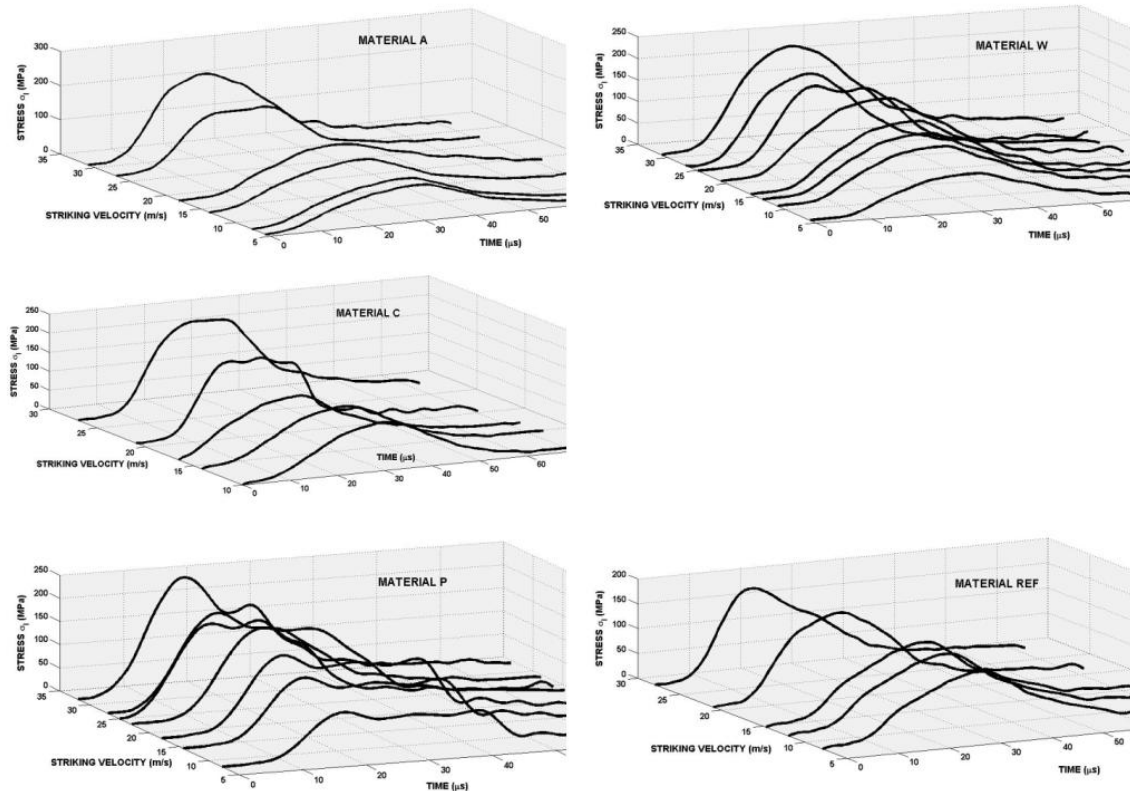


Figure3:Experimental records of the stress – time history recorded in the Hopkinson bar during the Taylor impact test.

One can see that there are some small differences in qualitative features of the stress time records for the tested materials. The specimen damage was observed nearly for all striking velocities. The only exception is the specimen of the material P at the striking velocity 7.8 m/s.

The effect of the striking velocity on the damage extent was evaluated at the three different times. These times are designated by the vertical lines: a, b and c in the Fig.2. The position a ($t = 14.28 \mu s$) occurs before the stress reaches its maximum value (amplitude). The position b ($t = 23.81 \mu s$) lies near of the stress pulse amplitude and the position c ($t = 52.38 \mu s$) nearly corresponds the end of the loading. The damage of the specimen which develops during the stress rising is shown in the Fig.4a.

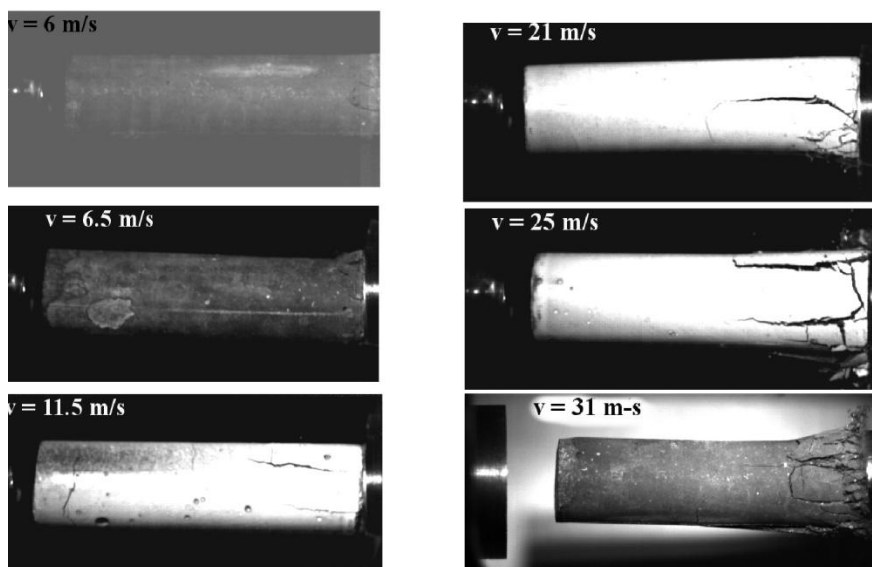


Figure4a:the development of the specimen damage at different striking velocities. Position a. Material W.The impact comes from the left side.

At the low striking velocities the damage starts near of the contact between the specimen and elastic bar. The specimen damage occurs in form of cracks at the specimen – bar interface. The increase of this velocity leads to the development of these „axial“ cracks. Their origin is probably caused by the stress connected with the specimen radial extension. The increase of the striking velocity leads to the more extensive damage of the frontal part of the specimen. At the highest used striking velocity the extensive specimen damage of the frontal part of the specimen was reported. Nearly no spall damage of the specimen was observed. The only exception is damage for the striking velocity = 11.5 m/s when some incipient spall at the rear part of the specimen was observed.

The specimen damage occurring near of the stress pulse maximum is documented in the Fig.4b.

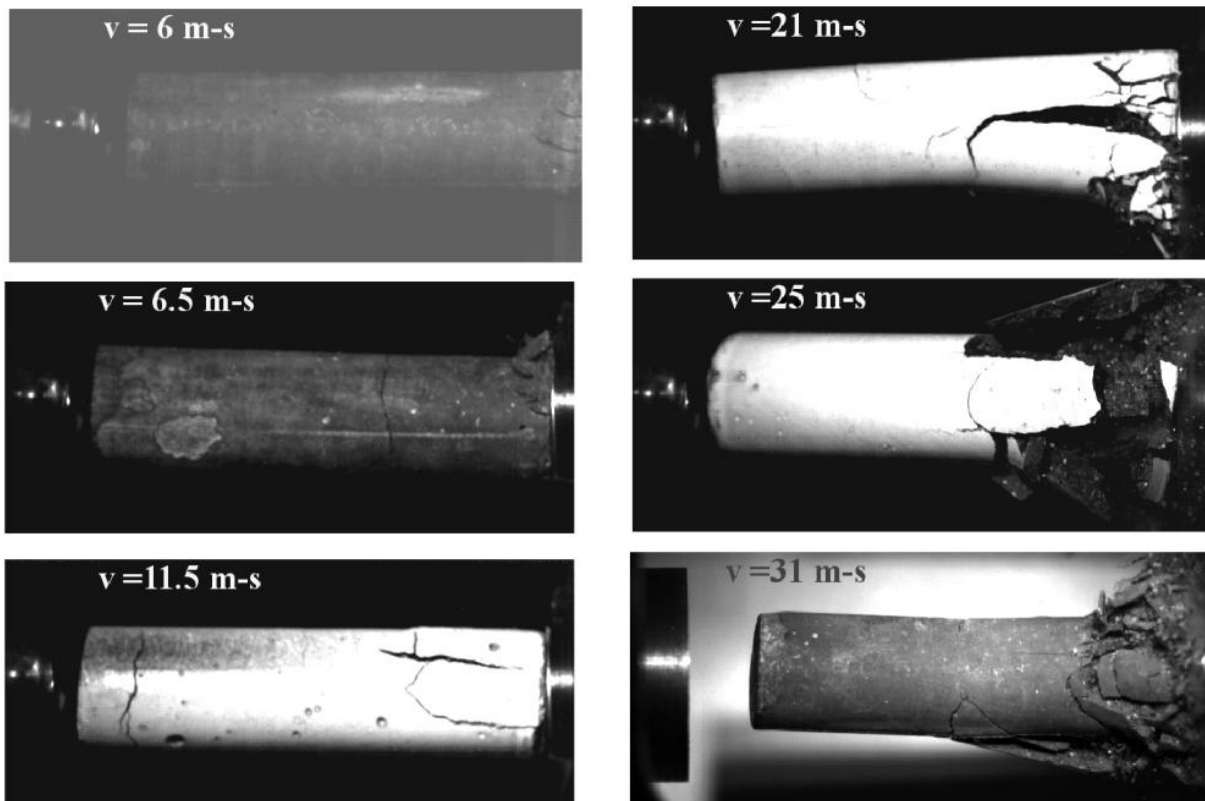


Figure4b: The development of the specimen damage at its different striking velocities. Position b. Material W.

It is evident that the increase of the stress leads to the growth of the damage shown in the previous Fig.4a and to the development of the spall damage.

The effect of the striking velocity on the specimen damage development at the end of the loading is documented in the Fig. 4c.

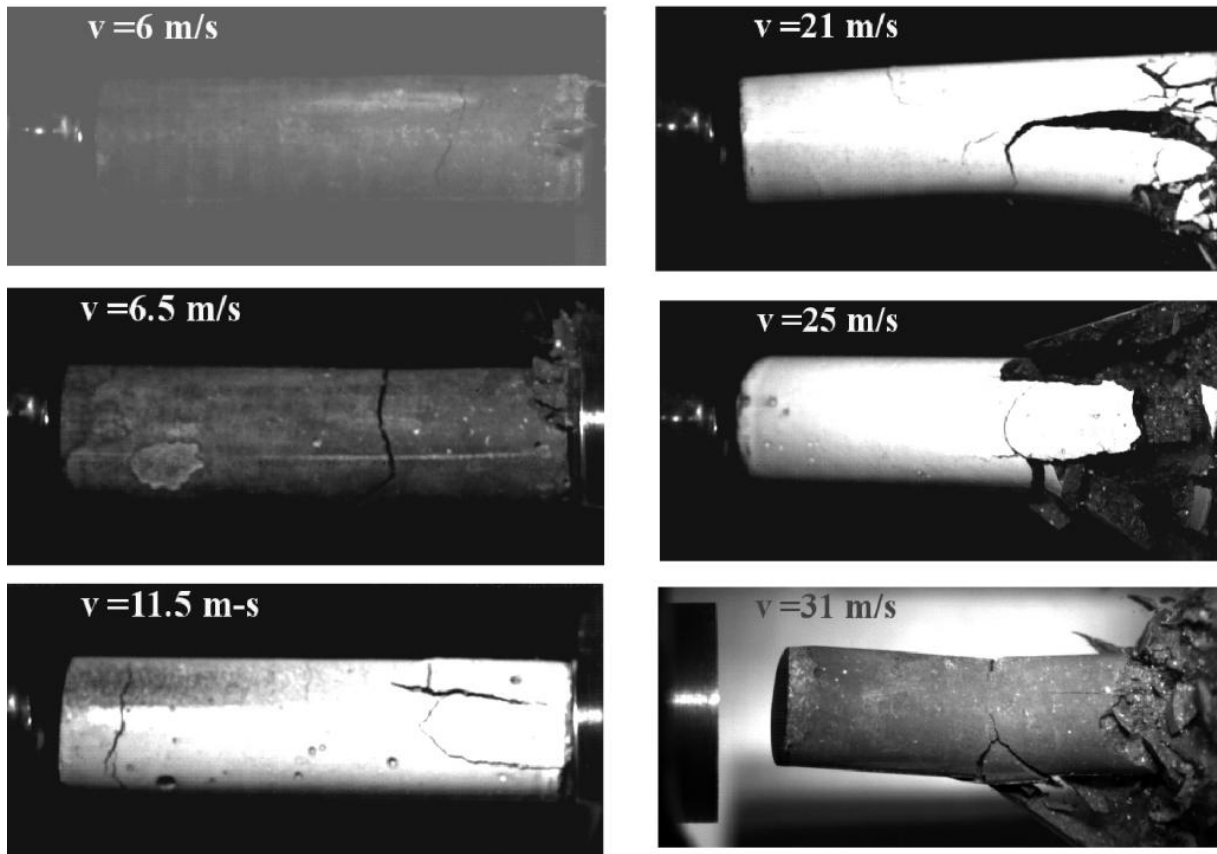


Figure4c: The development of the specimen damage at its different striking velocities. Position c. Material W.

The spall of the specimen starts at the minimum of the impact velocity. The small increase in the striking velocity leads to significant increase in the spall extent. The spall fracture may be also reported for the velocity of 31 m/s. The occurrence of the spall fracture for remaining impact velocities, i.e. 21 and 25 m/s is not to evident. At the small striking velocities the specimen damage at the impacted face is of small extent. The main damage is than in form of the spall.

Spall fracture damage was also reported for the specimen striking the Hopkinson bar with velocity 16 m/s. The development of the damage of this specimen is shown in the Fig.5.

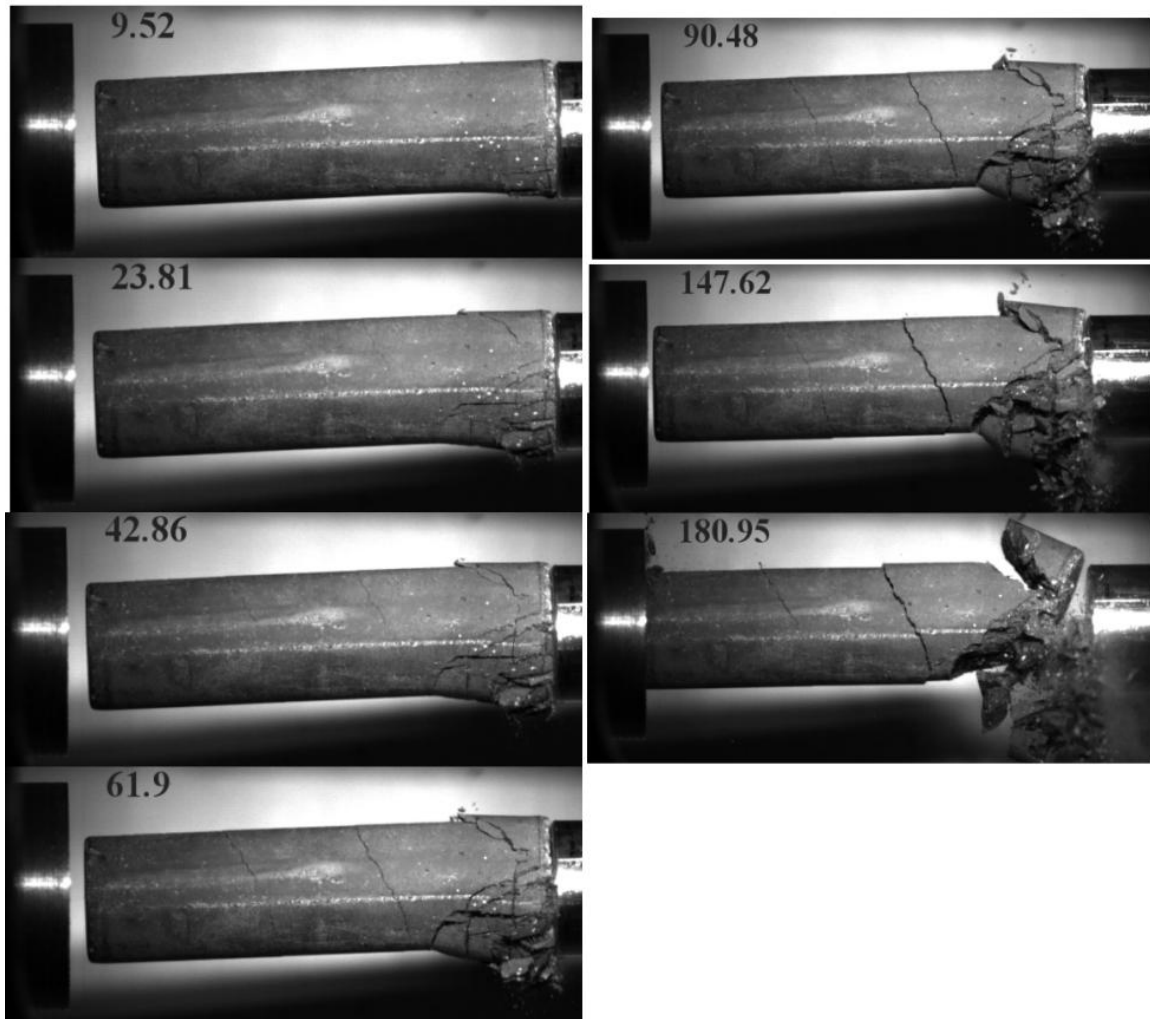


Figure5:High- speed photographic sequence of Taylor experiment performed at impact velocity 16 m/s. Labels indicate time (in μ s) after impact.Striking velocity = 16 m/s.Material W.

The specimen damage starts at the impacted face of the specimen. The extent of this damage grows in time and it is followed by the spall damage which starts between 42.86 and 61.9 μ s. The remaining two figures corresponds to the back specimen movement. During this movement the separation of the specimen along the spall plane is visible.

The stress pulse can be characterized by three parameters: maximum of the stress (amplitude), σ_{Im} , impulse I and energy w_I described in the chapter 2. In the Fig.6 the dependence of the stress pulse amplitude on the striking velocity is plotted.

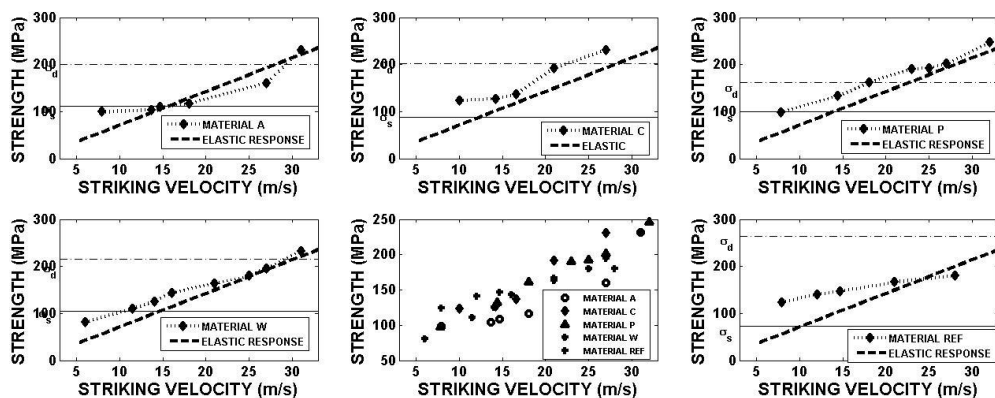


Figure6: Effect of the specimen striking velocity on the stress pulse amplitude.

The stress pulse maximum increases with the striking velocity. For the brittle material, this peak stress is defined as the dynamic compressive strength. [23]. If the specimen remains undamaged the maximum of the stress, σ_{max} , reported in the Hopkinson (elastic) bar can be estimated using one dimensional elastic wave theory [22]. According to this theory the maximum of the stress depends on the striking velocity V_o as:

$$\sigma_{max} = \frac{A_s Z_s Z_b}{A_s Z_s + A_b Z_b} V_o \dots \dots \dots (1)$$

where A is the cross- sectional area and Z is the acoustic impedance and the subscripts „s“ refers to the striker and „b“ the Hopkinson bar. In our experimental arrangement $A_s = A_b$. In the Fig.6 the maximum values of stress evaluated using Eq. (5) are plotted. The value of concrete acoustic impedance $Z_s = 8.62$ MPas/m was used [21]. Using this value of Z_s the Eq. (5) is:

$$\sigma_{max} = 7.118 V_o \dots \dots \dots (2)$$

The experimental points V_o, σ_{max} can be fitted as:

$$\sigma_{max} = a + b V_o \dots \dots \dots (3)$$

Parameters a, b are given in the Table III.

Table III. Parameters of the Eq. (7). R^2 is the square of the correlation between response values and predicted values.

MATERIAL	a (MPa)	b (MPas/m)	R^2
REF	105.4	2.767	0.9835
A	35.1	5.424	0.8469
W	45.72	5.719	0.9832
P	49.96	5.923	0.9824
C	38.92	6.917	0.9191

If we take parameter b as a measure of the strength rate sensitivity the order of the materials is:

$$REF, A, W, P, C \dots \dots \dots (4)$$

The rate sensitivity of the damaged specimens is lower than in the case of pure elastic response. In the given figure the values of static compressive strength, σ_s , and dynamic compressive strength, σ_d , are also shown. It is evident that with exception of striking velocity 31 m/s the values of the compressive strength evaluated of basic material REF is much lower in comparison with fibre reinforced materials. The rate dependence of the strength of material A is more complicated. With exception of material A, the values of maximum stress reported in the Fig.6 lie mostly above the line $\sigma_{max} (V_o)$.

The sensitivity of the compressive strength to the loading rate is higher for the fibre reinforced concrete than for the basic material. With the exception of the material A, all fibre reinforced materials exhibit higher values of the stress pulse amplitude, i.e. dynamic strength, than the unreinforced material (REF). Very similar conclusions were reported for the impulse and energy – see Figs. 7 and 8.

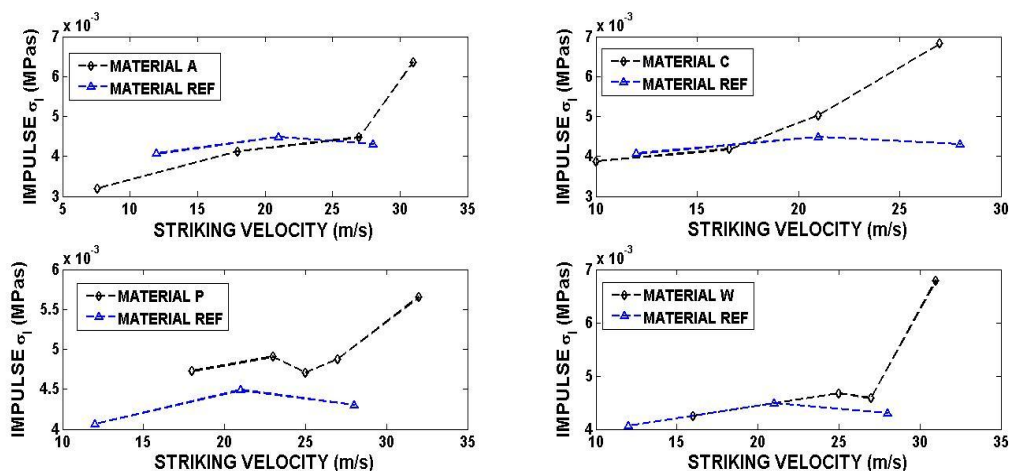


Figure7: Effect of the specimen striking velocity on the impulse of $\sigma_1 (t)$.

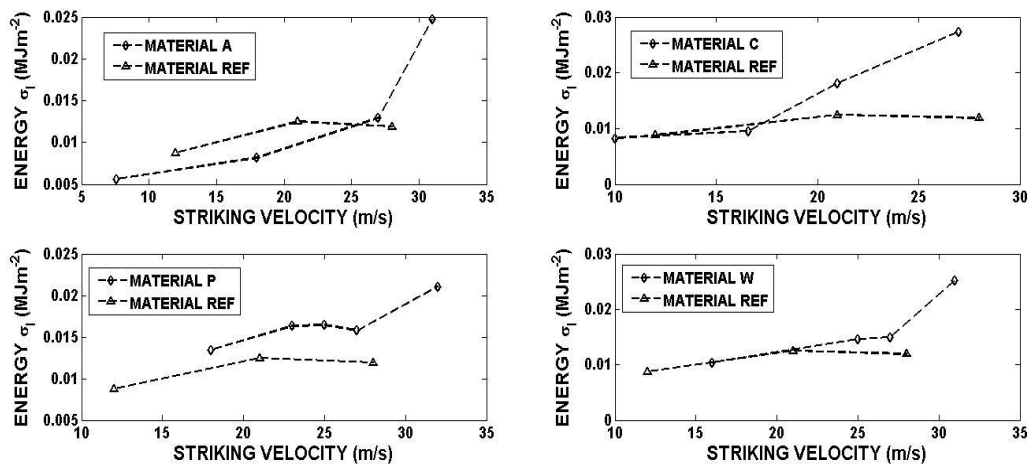


Figure8: Effect of the specimen striking velocity on the energy of $\sigma_I (t)$.

Owing to scatter of data the mutual comparison may be performed for the same value of striking velocity. This comparison was performed for the striking velocity $v = 27$ m/. The characteristics of the material response in the time domain are displayed in the Fig.9.

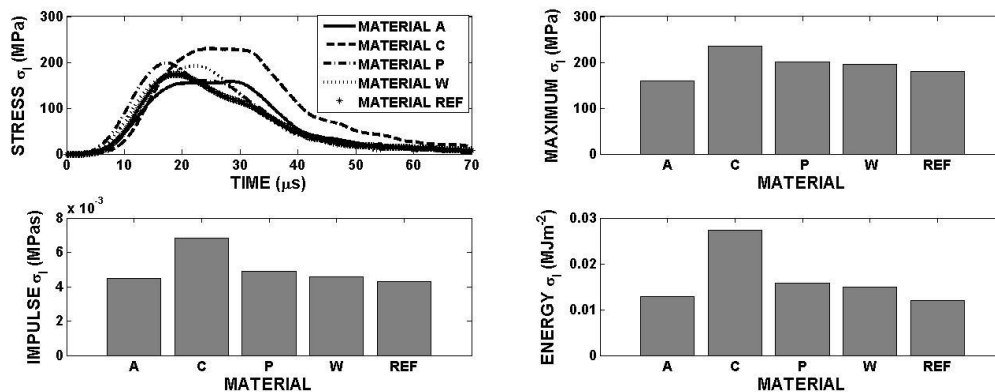


Figure9: Comparison of different stress pulse characteristics of the tested materials. Striking velocity = 27 m/s.

Results show that the order of tested materials from the lowest to the highest value of the stress pulse maximum (dynamic strength) is similar as in the case of the strength rate sensitivity, i.e. :

$$A, REF, W, P, C \dots \dots \dots (5)$$

The maximum value of the compressive strength exhibits the material C (carbon fibres). The relative high value of dynamic compressive strength of material P (polypropylene fibres) is unexpected because most of up to known results show that the effect of addition of these fibres exhibits insignificant effect on the compressive strength owing to their low elastic modulus[24].

In the Fig.10 the values of the dynamic compressive strength evaluated using Taylor test and values of static strength and dynamic strength are plotted. The static and dynamic strengths (SHPB) were obtained in [17].

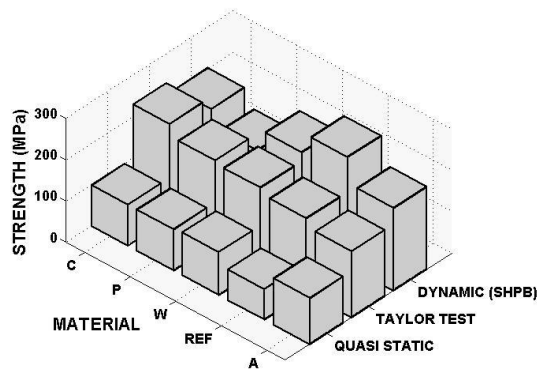


Figure10: Compressive strength of the tested materials obtained using different experimental method.

The dynamic compressive strength (SHPB) was evaluated at the strain rate about 1600 s^{-1} .

The order of materials according to the values of their compressive strength is:

Quasi static loading:

$$\text{REF,C,P,W,A} \dots\dots\dots(6)$$

Dynamic (SHPB method):

$$\text{P,A,C,W,REF} \dots\dots\dots(7)$$

The use of the different methods of the dynamic loading, i.e. Taylor test and SHPB test leads to quite different results - see Eqs. (5) and (7).

In order to give some more detail view on the behaviour of tested materials the development of the specimen damage was evaluated at the times a, b, c - see Fig.2. Results are presented in the Figs.11a-e.

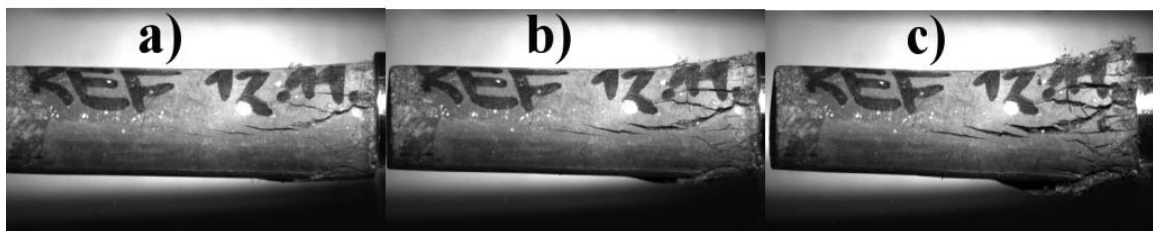
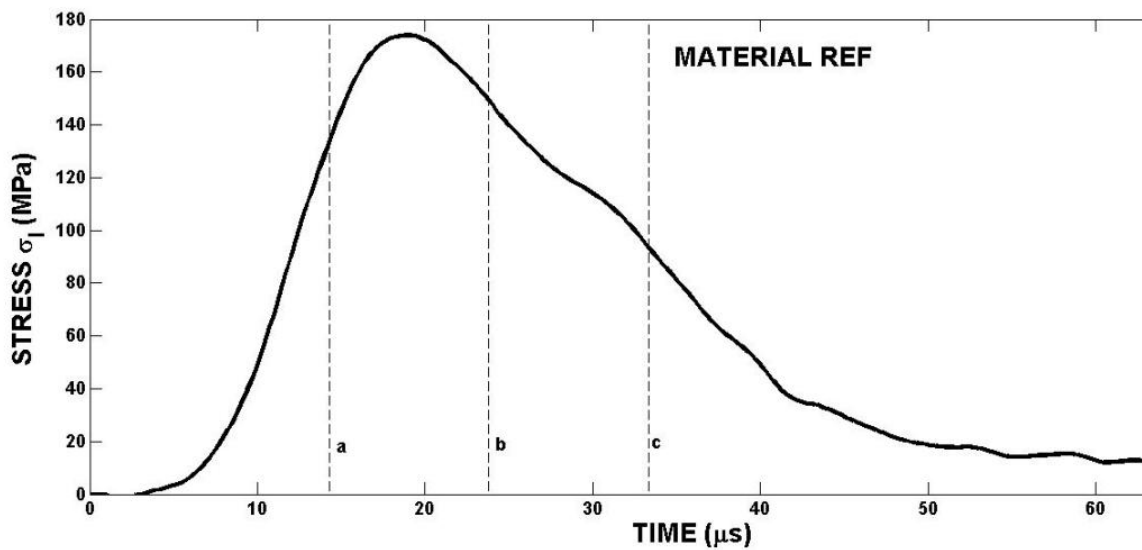


Figure11a: Development of the specimen damage during impact loading of the specimen. Material REF.Striking velocity 27 m/s.

The damage develops in form of some axial cracks. The distribution of the damage is not symmetric along the specimen axis. These cracks can be a consequence of the specimen radial expansion at the specimen – Hopkinson bar interface. No spall damage was observed. It means the damage of the specimen leads to the decrease of the stress below the spall strength.

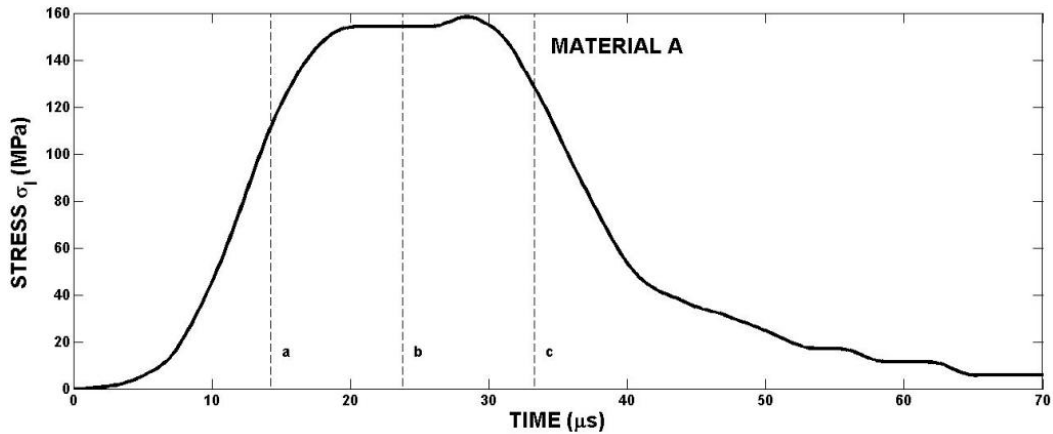


Figure11b: Development of the specimen damage during impact loading of the specimen. Material A. Striking velocity 27 m/s.

The specimen damage is significantly lower than in the previous case. The cracks look like a spall.

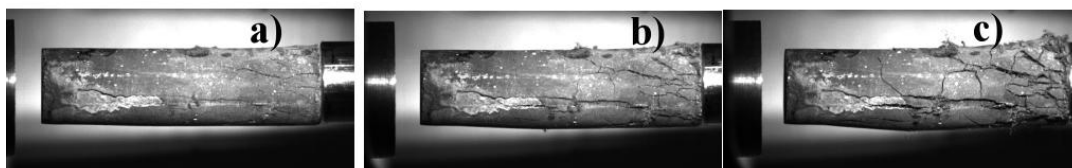
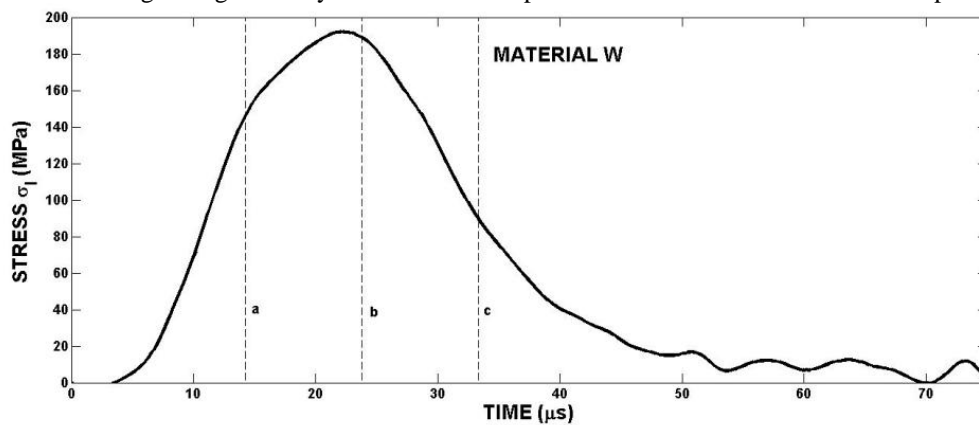


Figure11c: Development of the specimen damage during impact loading of the specimen. Material W. Striking velocity 27 m/s.

The specimen damage is in the form of a fragmentation, namely in the frontal part of the specimen.

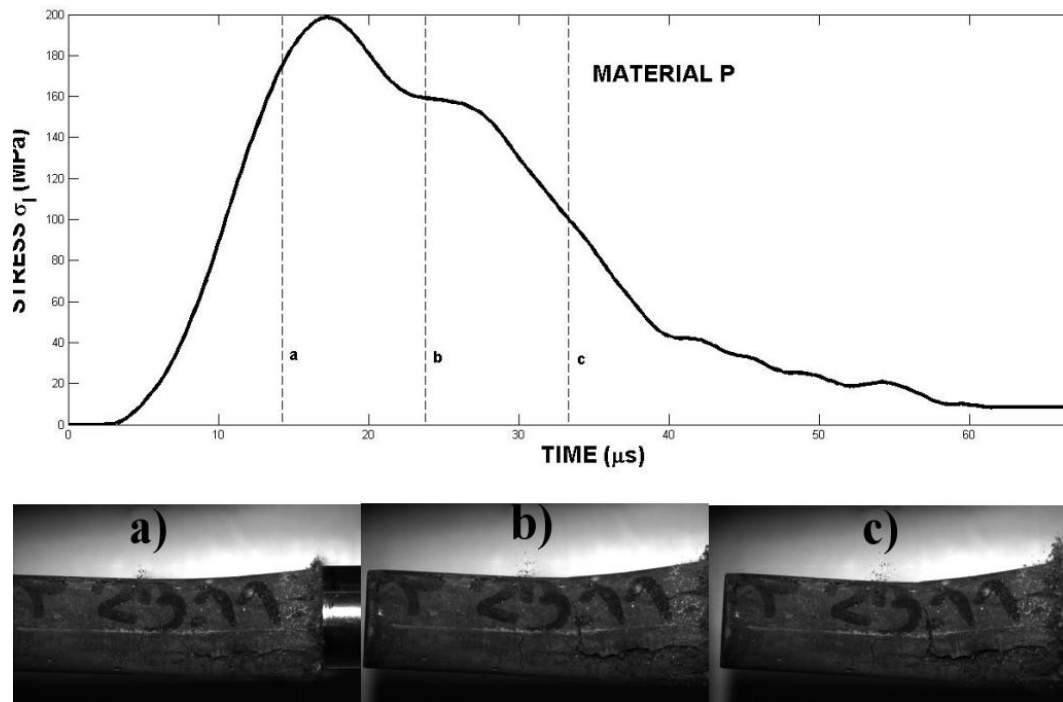


Figure11d: Development of the specimen damage during impact loading of the specimen. Material P. Striking velocity 27 m/s.

The specimen damage is lower than in the foregoing cases. The damage is in the form of some thin axial cracks. The specimen appear to expand as comminuted material moves radially outwards.

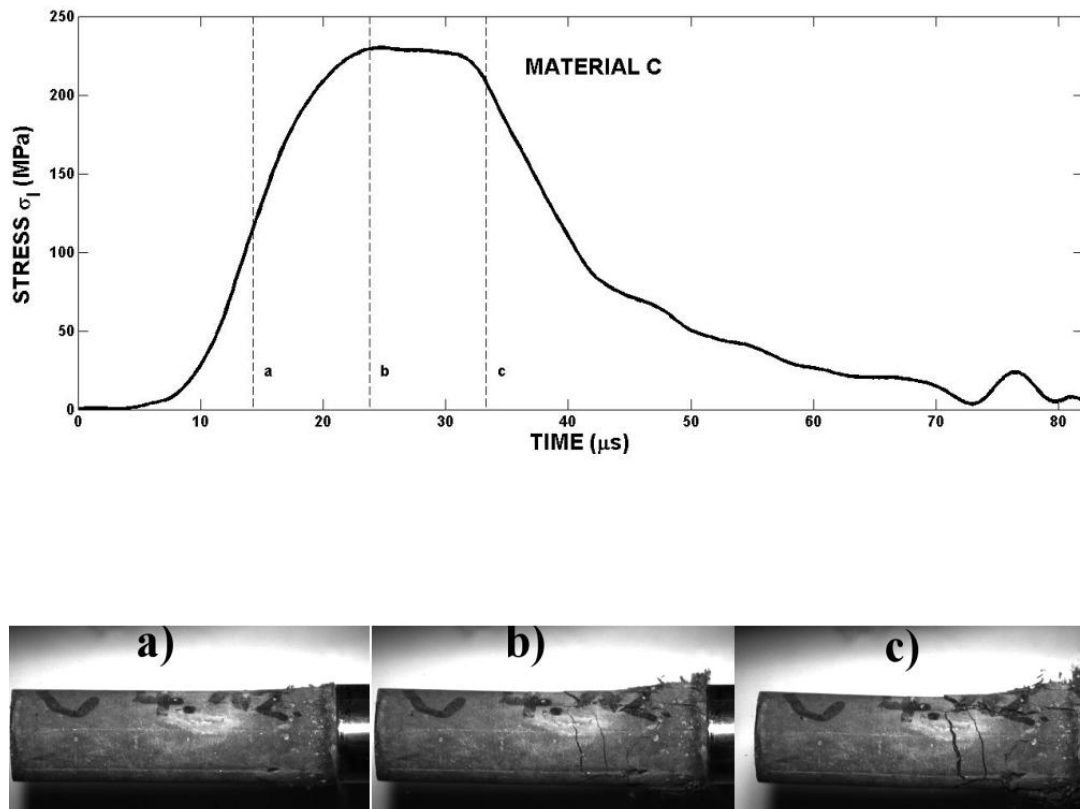


Figure11e: Development of the specimen damage during impact loading of the specimen. Material C.

The specimen damage develops mostly in the form of a multiple spall fracture. Some comminution at the impact face of the specimen may be also reported.

Results presented in the Figs 11a-e show that the qualitative features of the specimen damage are different for the different materials. The extent of the final specimen damage reported in time 52.38 μ (position c) shows that the material A is more resistant to the impact loading than the material W. It means there is some change in the order of materials given by the Eq. (9). The Taylor impact of the specimen on the elastic bar leads to its spall damage and more or less fragmentation of its frontal part.

The effect of the striking velocity on the final specimen damage is presented in the Figs. 12a-c.

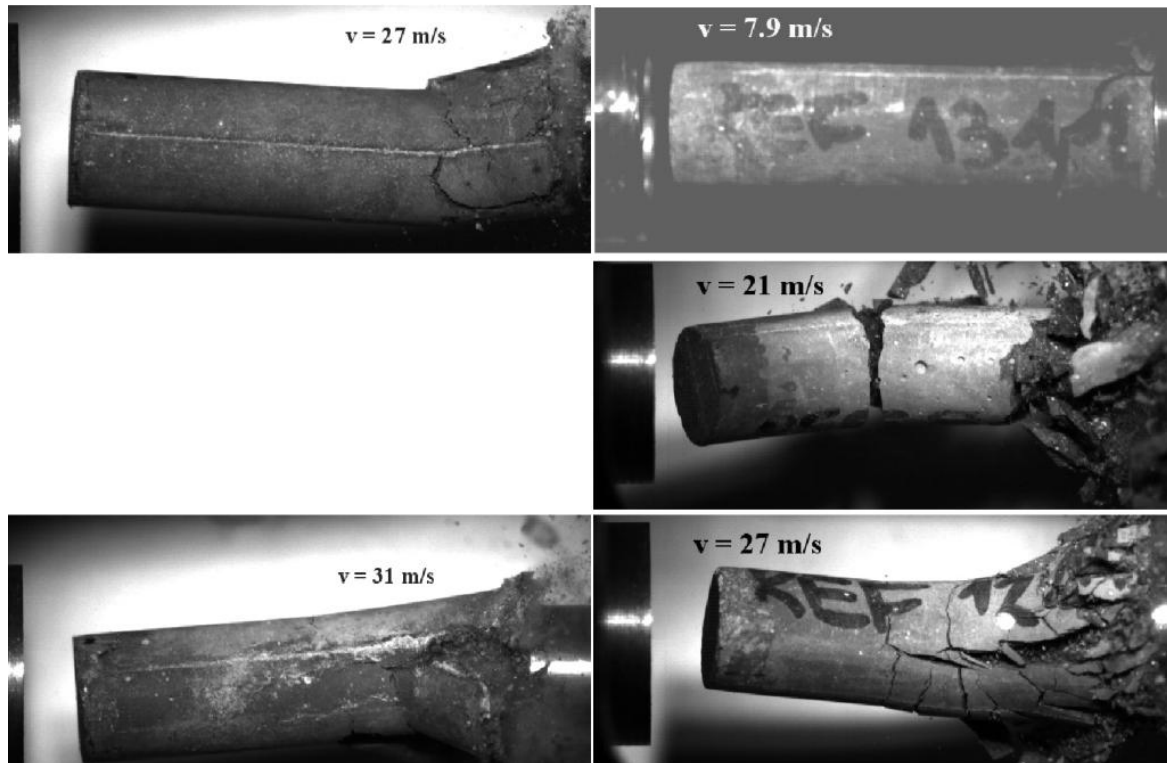


Figure 12a: Final damage of the specimen after Taylor impact. Material A (left part) and material REF (right part).

One can see the final damage of the specimen (material A) exhibits spall fracture. If take into account the results shown in the Fig. 11b it is obvious that the spall was increased namely during the unloading part of the stress pulse. The material REF is damaged in the form of a fracture near of the contact specimen –bar. The increase in the striking velocity leads to the development of the spall fracture and heavily damaged frontal part of the specimen. The next increase in the striking velocity leads to some comminution of materials of the specimen frontal part and to the development of a multiple spall fracture.

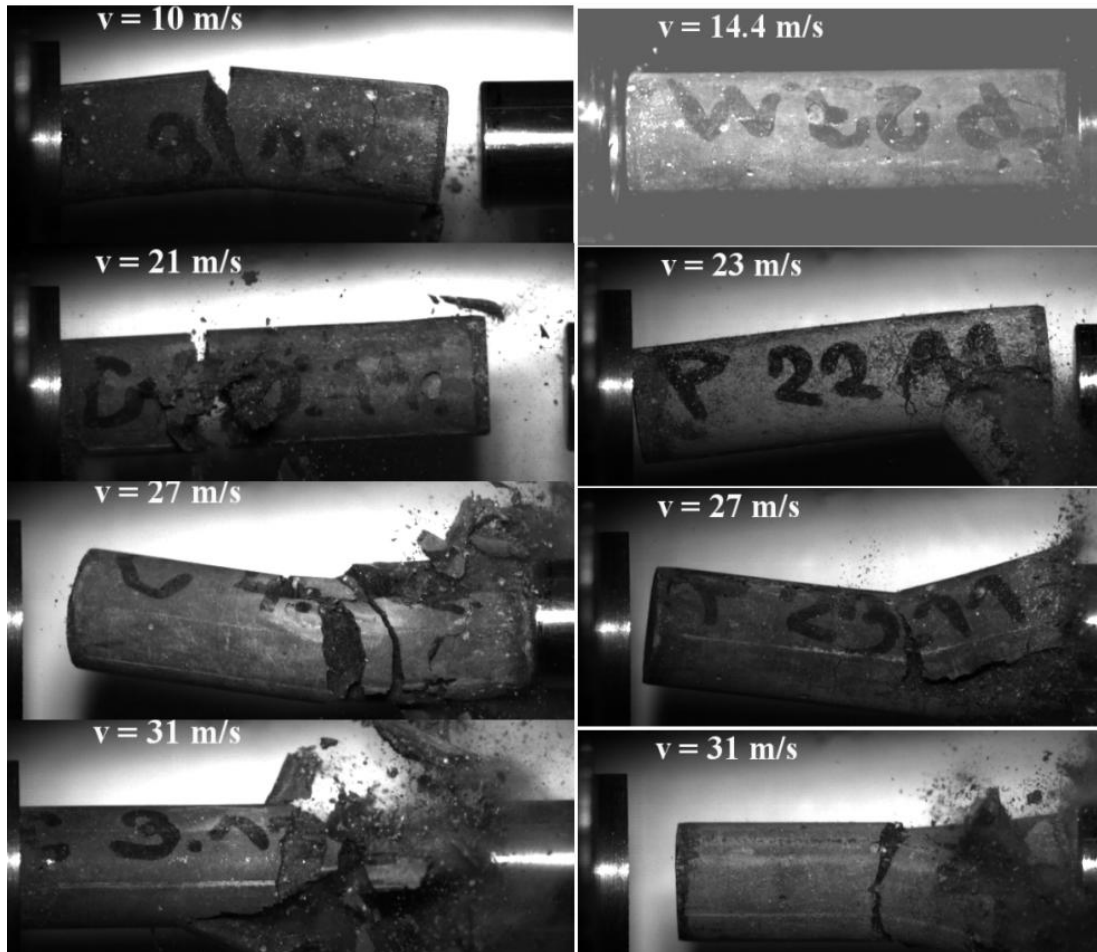
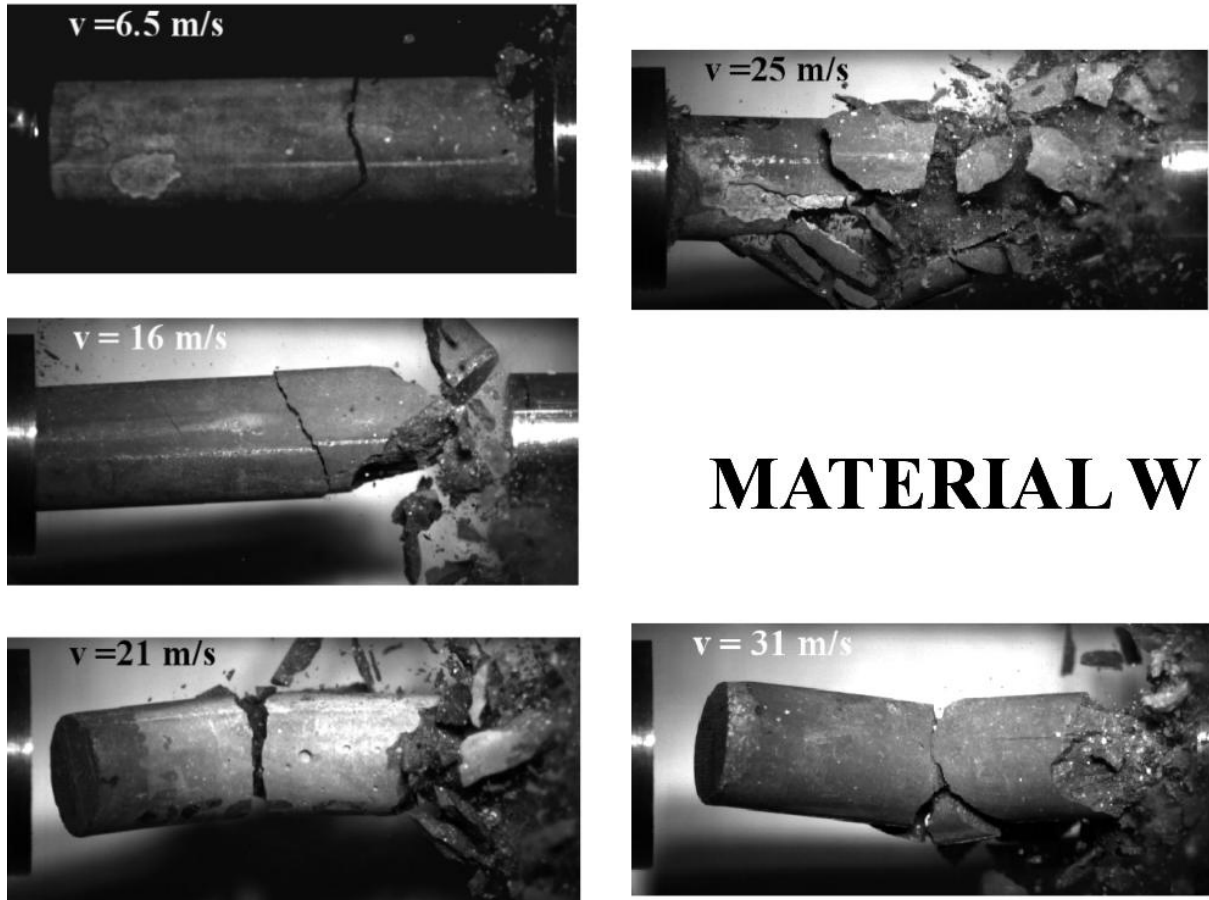


Figure12b: Final damage of the specimen after Taylor impact. Material C (left part) and material P (right part).

At the striking velocity up to 21 m/s, the damage of material C (carbon fibre) is in the form of spall fracture with nearly no damage of the specimen frontal part. The increase in the striking velocity leads to the damage of the frontal part and to the spall fracture. The spall fracture of the specimen made from material P (polypropylene fibres) starts at the higher striking velocity than that at specimen made from the material C. This observation is in agreement with some findings that the Polypropylene fibres can improve the tensile strength of the concrete [24]. The damage increase with the striking velocity and it is similar like in the case of material C. Its extent is lower. The addition of polypropylene fibres leads to lower damage extent than in the case of addition of carbon fibres.



MATERIAL W

Figure12c: Final damage of the specimen after Taylor impact. Material W.

The damage of the specimen starts as the spall fracture at the very low striking velocity. The increasing of this velocity is accompanied with growth of the frontal specimen damage. Some exception represents the specimen impacted by the velocity 25 m/s when the whole specimen fragmentation was observed.

The results of the brief description of the specimen damage development show that the response of material to dynamic loading during the Taylor impact test is affected both the compressive and tensile mechanical properties. The compressive strength affects the damage of the frontal part of the specimen and the tensile strength determines material resistivity to the spall fracture.

IV. CONCLUDING REMARKS.

In the given paper, the impact - resistance behaviour of fibre reinforced concrete was studied using the Taylor impact test. Four different fibres were used: carbon, polypropylen, aramide and wollastonite. The following conclusions can be drawn:

1. The values of dynamic compressive strength evaluated from the Taylor test lie between value of the static compressive strength and dynamic compressive strength obtained using Split Hopkinson Pressure Bar method.
2. The dynamic compressive strength increases linearly with the striking velocity. The sensitivity of this strength to the loading rate is highest for concrete reinforced by the carbon fibres (Material C). Very similar sensitivity exhibits concrete reinforced by the polypropylene fibres (Material P). The sensitivity of all fibre reinforced composites is significantly higher than that of the unreinforced concrete.
3. Minimum increase of the compressive strength in comparison with unreinforced concrete exhibits concrete reinforced by addition of aramidfibres. Values of dynamic compressive strength of all tested materials lie above the stress corresponding to the pure elastic response of the unreinforced concrete.
4. The study of the specimen damage during the loading shows that there is damage of the specimen frontal part which is affected namely by the compressive strength and the spall fracture which is affected by the tensile strength. Results of the preliminary observation confirm that the best improvement in the tensile strength and thus the spall resistivity affects the addition of the

polypropylene fibres. The minimum resistance to the spall exhibits concrete reinforced by the wollastonite fibres (Material W).

5. The response of the material during the Taylor impact test is affected both by the compression and tensile strength characteristics. It means that this test is convenient namely for the validation of constitutive equations used in numerical codes.

ACKNOWLEDGEMENT

This research was supported by the European Regional Development Fund under Grant No. CZ.02.1.01/0.0/0.0/15_003/0000493 (Centre of Excellence for Nonlinear Dynamic Behavior of Advanced Materials in Engineering).

REFERENCES

- [1]. Wu,Z.M., Shi,C.J, He,W. and Wang,D.H.,(2017).” Static and dynamic compressive properties of Ultra-high performance concrete (UHPC) with hybrid steel fibre reinforcements”, *Cement Concr. Compos.* 79 , 148–157.
- [2]. Lai,Z.J. and Sun, W.,(2009).”Dynamic behaviour and visco-elastic damage model of ultra-highperformance cementitious composite”, *Cement Concr. Res.* 39 (11),1044–1051.
- [3]. Mastali,M. A., Dalvand, A.and Sattarifard,A.R.,(2016).”The impact resistance and mechanical properties of reinforced self-compacting concrete with recycled glass fibre reinforced polymers”, *J. Clean. Prod.* 124, 312–324.
- [4]. Doo-Yeol Yoo and Nemakumar Banthia,(2019).” Impact resistance of fibre reinforced concrete - A review”, *Cement and Concrete Composites* 104, 103389.
- [5]. Li,Q. and Meng, H.,(2003).”About the dynamic strength enhancement of concrete-like materials in a split Hopkinson pressure bar test”, *Int. J. Solids Struct.* 40, 343-360.
- [6]. Asprone,D., Cadoni,E. and Prota,A.,(2009).” Experimental analysis on tensile dynamic behaviour of existing concrete under high strain rates”, *ACI , J.* 106,106–1131.
- [7]. Taylor G.I .,(1948).” The use of flat ended projectiles for determining dynamic yield stress”,*Proc R Soc London A* , 194 , 289-99.
- [8]. Emrah Konokman,H.E.,Murah Coruh,M.and Altan Kayran,(2011).”Computational and experimental study of high-speed impact of metallic Taylor cylinders”,*Acta Mech*220, 61-85.
- [9]. Martin,M.,Shen,T.and Thadhani,N.,(2008).” Instrumented anvil-on-rod impact experiments for validating constitutive strength model for simulating transient dynamic deformation response of metals”,*Mater Sci Eng ,A*494 ,416-424.
- [10]. Briscoe,B.J., Hutchings,I.M.,(1976).”Impact yielding of high density polyethylene”,*Polymer* 17,1099-102.
- [11]. Vartanov, M.A. Dmitrieva,T.A. and Romanchenko,V.I.,(1990).” Dynamic properties of polycarbonate with impact of a cylinder on an obstacle”, *Combust Explo Shock Waves* 25,490-492.
- [12]. Rae,P.J.,Brown ,E.N.,Clements,B.E.and Dattelbaum,D.M.,(2005).”Pressure induced phase change in poly (tetrafluoroethylene) at modest impact velocities”,*J Appl Phys*,9,1-8.
- [13]. Zhang,Q.B. and Zhao,J.,(2014).”A review of dynamic experimental techniques and mechanical behaviour of rock materials”, *Rock Mech Rock Eng*, 47,1411–1478.
- [14]. G.R.Willmott,G.R. and Radford,D.,(2005). “Taylor impact of glass rods”, *J Appl. Physics*, 97(9) ,93522-1-8.
- [15]. Ruggiero,A.,Iannitti,G.,Bonora,N. and Ferraro,M.,(2012).” Determination of Johnson-Holmquist constitutive model parameters for fused silica”,*EPJ Web of Conferences*26,04011.
- [16]. Brar,N.S, Proud,W.G. and Rajendran,A.M.,(2004).” Ceramic Bar Impact Experiments for Improved Material Model”, *AIP Conference Proceedings* 7006,727 .
- [17]. Drdlová,M.,Popovic,M. and Čechmánek, R.,(2018).”High Strain Rate Compressive Behaviour of Micro-Fibre Reinforced Fine Grained Cementitious Composite”, *Solid State Phenomena*, 276,140-147.
- [18]. Popovič,M., Buchar,J. and Drdlová,M.,(2018).”High strain rate behavior of fiber reinforced concrete”, *EPJ Web of Conferences* 183,02012.
- [19]. Grey, J.M. and Gordon,J.W.,(1978).” Perceptual effects of spectral modifications on musical timbres”, *J. Acoust. Soc. Am.*, 63 (5), 1493-1500.
- [20]. Lopatnikov,S.L.,Gama,B.A. et al.,(2003).” Dynamics of metal foam deformation during Taylor cylinder / Hopkinson bar impact experiment”, *Composite Structures*,61,61-71.
- [21]. Brara,A. and Klepaczko,J.R.,(2006).” Experimental characterization of concrete in dynamic tension”, *Mech Mater* ,38,253–267
- [22]. Johnson,W.(1973).” Impact Strength of Materials”,Ed. Edward Arnold, 1-37.
- [23]. Bless,S. and Tolman,J.,(2009).” Impact Strength of Glass and Glass Ceramics”,*AIP Conference Proceedings*1195, 1421 , doi: 10.1063/1.3295078.
- [24]. Song,P.S.,Hwang,S. and Sheu,B.C.,(2005).”Strength properties of nylon- and polypropylene fiber-reinforced concretes”, *Cement Concr. Res.* 35 (8),1546–1550.

Jaroslav Buchar. "Taylor Impact of Fibre Reinforced Concrete Bars." *International Journal of Modern Engineering Research (IJMER)*, vol. 10(10), 2020, pp 30-45.